Planet. Space Sci., Vol. 23, pp. 1669 to 1679. Pergamon Press, 1975. Printed in Northern Ireland

AN AURORAL *F*-REGION STUDY USING *IN SITU* MEASUREMENTS BY THE ATMOSPHERE EXPLORER-C SATELLITE

MARSHA R. TORR and D. G. TORR
National Astronomy & Ionosphere Center, Cornell University, Ithaca, New York 14850, U.S.A.
Space Physics Research Laboratory, University of Michigan, Ann Arbor, Michigan 48105, U.S.A.
National Institute for Telecommunications Research of C.S.I.R., P.O. Box 3718, Johannesburg, South Africa

R. A. HOFFMAN
Planetary Aeronomy Branch, Goddard Space Flight Center, Greenbelt, Maryland 20771, U.S.A.

W. B. HANSON and J. H. HOFFMAN
Institute for Physical Science, University of Texas at Dallas, Richardson, Texas 75080, U.S.A.

W. K. PETERSON
Department of Chemistry, Johns Hopkins University, Baltimore, Maryland 21218, U.S.A.

and

J. C. G. WALKER
National Astronomy & Ionosphere Center, Arecibo Observatory, Arecibo, Puerto Rico 00612, U.S.A.

(*Received* 10 *June* 1975)

Abstract—On 14 July 1974 the Atmosphere Explorer-C satellite flew through an aurora at *F*-region altitudes just after local midnight. The effects of the particle influx are clearly evident in the ion densities, the 6300 Å airglow, and the electron and ion temperatures. This event provided an opportunity to study the agreement between the observed ion densities and those calculated from photochemical theory using *in situ* measurements of such atmospheric parameters as the neutral densities and the differential electron energy spectra obtained along the satellite track. Good agreement is obtained for the ions O_2^+, NO^+ and N_2^+ using photochemical theory and measured rate constants and electron impact cross sections. Atomic nitrogen densities are calculated from the observed $[NO^+]/[O_2^+]$ ratio. In the region of most intense electron fluxes (20 erg cm^{-2} sec^{-1}) at ~280 km, the N density is found to be between 2 and 7 $\times$ 10^7 cm^{-3}. The resulting N densities are found to account for approx. 60% of the production of N^+ through electron impact on N and the resonant charge exchange of $O^+(^2P)$ with $N(^4S)$. This reaction also provides a significant source of $O(^1S)$ in the aurora at *F*-region altitudes. In the region of intense fast electron influx, the reaction with atomic nitrogen is found to be the main loss of $O^+(^2P)$.

1. INTRODUCTION

On 14 July 1974 at 00:48 LT the Atmosphere Explorer-C satellite (see Dalgarno *et al.*, 1973) entered a latitudinally—varying diffuse aurora at *F*-region altitudes. It emerged from the aurora at a local time just prior to morning twilight. The total electron energy input together with the variation along the satellite track of altitude, invariant latitude, and solar zenith angle are shown in Fig. 1. The effects of particle precipitation are clearly evident in the ion densities, 6300 Å airglow, and the electron (T_e) and ion (T_i) temperatures shown in Fig. 1. This provided an opportunity to study the agreement between observed ion densities and those calculated from photochemical theory using *in situ* measurements of ionic and neutral composition, T_e, T_i, and electron flux at each point along the track together with current values for reaction rates.

We do not know of any other study comparing observed and calculated ion densities in an aurora at *F*-region altitudes. Other auroral studies in recent years (Narcisi and Swider, 1970; Donahue *et al.*, 1970; Narcisi *et al.*, 1974; Swider and Narcisi, 1974) have dealt with rocket observations in the *E* and lower *F* regions where the energy deposition is a maximum. These studies have not had the benefit of *in situ* measurements of the

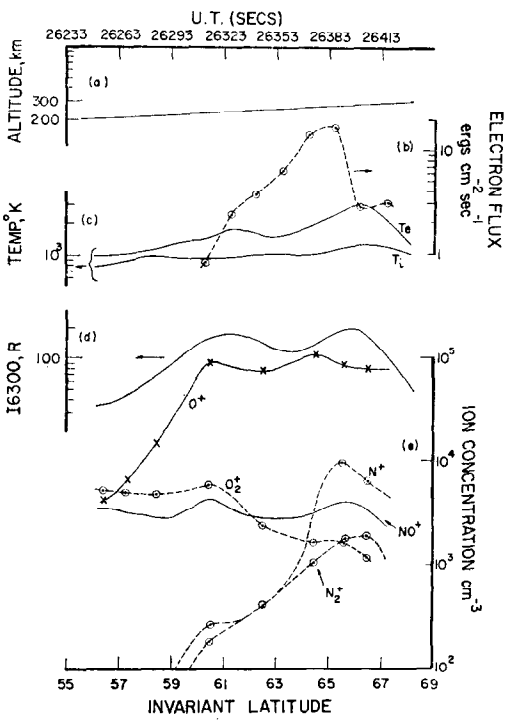

FIG. 1. VARIATION OF (a) SATELLITE ALTITUDE, (b) ELECTRON ENERGY INPUT, (c) T_e AND T_i, (d) 16300 AND (e) ION DENSITIES THROUGH THE AURORA AS A FUNCTION OF UT AND INVARIANT LATITUDE

neutral atmosphere or particle fluxes. A study of the ionization response times to the particle source has been made by Jones and Rees (1973).

In this work we shall consider the altitude region from 200 to 300 km. The upper limit is determined by two factors. Although photoelectrons from atomic oxygen excited by He II radiation are visible at altitudes above 250 km, twilight effects do not begin to contribute until 320 km on this orbit. Transport is also a factor at higher levels.

The satellite has the capability of operating in either a spinning or oriented mode. On this pass the satellite was spinning (1/15 rev/sec). This mode is advantageous because it provides good information on the pitch angle distribution of the precipitating electrons, the major source of the auroral effects to be investigated. However, in the spinning mode the ion density measurements are degraded in spatial resolution and accuracy.

2. FAST ELECTRON FLUXES

Fast electron fluxes are measured by two instruments on the AE-C. The energy range from 0·2 to 25 keV is covered by the low energy electron detector (LEE) described by Hoffman *et al.* (1973). Fluxes at lower energies are measured by the photoelectron spectrometer (PES) described by Doering *et al.* (1973, 1975). This instrument measured electrons in the energy range 1·5–97·5 eV on this orbit.

In studying this aurora, it is not possible for us to resolve altitudinal, latitudinal, and temporal variations. It is probable that the satellite passed at different altitudes through latitudinally varying precipitation. For convenience in what follows we shall identify portions of the data by referring to them in terms of universal time.

Figure 2 shows the flux energy spectra obtained on the 8 satellite spin cycles between 26,309 and 26,420 sec UT. Between 26,233 and 26,300 sec UT (56–60 Λ where Λ denotes invariant latitude) the electron fluxes were below instrument thresholds. From 26,300 to 26,380 sec UT (60–~65 Λ) the satellite passed through a diffuse auroral region in which the spectra were isotropic. Between 26,395 and 26,415 sec UT (66–67 Λ) the fluxes became more variable with pitch angle with the spin centered at 26,385 sec UT showing the most variation. In the case of the spin centered at

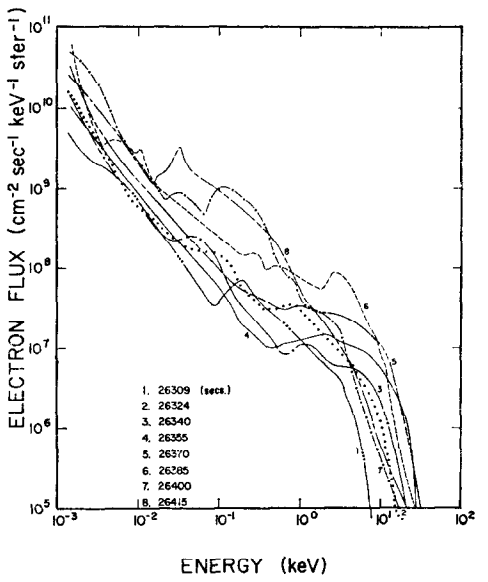

FIG. 2. ELECTRON ENERGY SPECTRA AT 15 SEC INTERVALS THROUGH THE AURORA. EACH SPECTRUM IS LABELLED IN TERMS OF THE UT AT THE CENTER OF THE 15 SEC INTERVAL IN WHICH THE MEASUREMENT WAS MADE.

The portion below 100 eV was measured by the PES and above 200 eV by the LEE instruments (see text). Spectra 1 to 5 are isotropic. Spectra 6 to 8 are anisotropic and the average flux over pitch angle at each energy is shown here.

26,400 sec UT the fluxes remained relatively isotropic above 1 keV, but became strongly field-aligned below 1 keV. For the three spins showing anisotropy, we have used the flux averaged over pitch angle at each energy. It is this average that is shown in Fig. 2. Figure 1 shows the integral over energy of the spectra in Fig. 2. After 26,415 sec UT (67 Λ) the satellite moved into the polar cap region, and the fluxes again fell to the threshold of the higher energy detector, and the low energy spectrometer measured spectra characteristic of the twilight airglow.

Both the total energy flux in Fig. 1 and the spectra in Fig. 2 were obtained with the higher energy particle detector looking into the upper hemisphere. The backscattered fraction of these electrons varied between 10 and 30%. The proton energy fluxes at these altitudes were less than 7% of the electron energy flux.

3. NEUTRAL ATMOSPHERE

On this pass the O, N_2 and He densities were measured by the open source neutral mass spectrometer (OSS) described by Nier *et al.* (1973). These densities are shown in Fig. 3.

On this section of the orbit the $[N_2]$ and the [O] show what appears to be a wave structure which is anticorrelated with that in [He] [Mauersberger, private communication, 1975]. On this pass O_2 densities were not measured (see Nier *et al.*, 1974a). However, Nier *et al.* (1974b) have established from passes on which $[O_2]$ and $[N_2]$ were measured simultaneously that the O_2 density is generally about 8% of the N_2 density at 200 km.

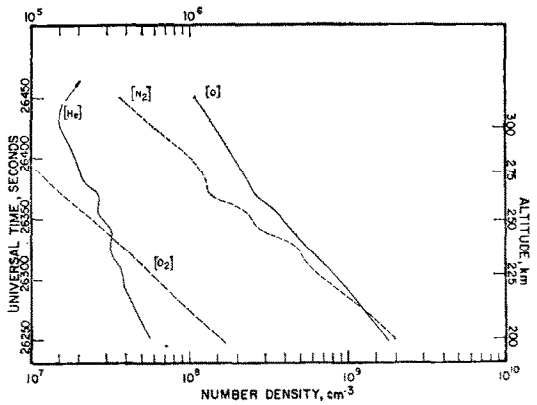

FIG. 3. ATOMIC OXYGEN, HELIUM AND MOLECULAR NITROGEN DENSITIES MEASURED ON ORBIT 2393 BY THE OPEN-SOURCE MASS SPECTROMETER ON AE-C. ALSO SHOWN IS THE $[O_2]$ OBTAINED AS DISCUSSED IN THE TEXT.

We have used a profile in agreement with this value.

Neutral temperatures (T_n) were measured by the neutral-atmosphere temperature experiment (NATE) described by Spencer *et al.*, (1973), but were not available above 237 km. At higher altitudes a model T_n was therefore, used with an exospheric temperature of 1100°K, consistent with the atomic oxygen densities (Carignan, private communication, 1975). The variations in the $[N_2]$ profile made it difficult to determine neutral temperatures from this constituent although generally $[N_2]$ should be a better parameter than [O] from which to derive T_n (Hays *et al.*, 1974).

4. COMPARISON OF THE ION COMPOSITION WITH PHOTOCHEMICAL THEORY

The ion densities were measured by the magnetic ion mass spectrometer (MIMS) described by Hoffman *et al.* (1973). The ion temperatures were measured by the retarding potential analyser (RPA) described by Hanson *et al.* (1973). The electron temperatures were measured by the cylindrical electrostatic probe (CEP) described by Brace *et al.* (1973). The temperatures T_i and T_e are shown in Fig. 1.

The reactions considered in the calculation of the density of each ionic constituent are listed in Table 1 and the reaction rates and branching ratios are listed in Table 2.

The electron impact cross-sections for ionization of N, N_2, O_2 and He are taken from Banks and Kockarts (1973) who have compiled these from measurements by Kieffer and Dunn (1966), Tate and Smith (1932), Rapp and Englander-Golden (1965) and Schram *et al.* (1965, 1969). In the case of O, we have used the values from Dalgarno and Lejeune (1971) to calculate the production rate of $O^+(^2P)$ and $O^+(^2D)$. Above 100 eV we used 22 and 38% of the total cross-section for ionization of O to obtain the $O^+(^2P)$ and $O^+(^2D)$ production rates respectively. We have assumed that 44% of the total O_2^+ ions are produced in the metastable $O_2^+(a^4\pi)$ state (Jones and Rees, 1973).

(a) NO^+ *and* O_2^+

In Fig. 4 we show the observed and calculated NO^+ and O_2^+ densities. The observed $[NO^+]/[O_2^+]$ ratios are given in Table 3. In calculating the densities shown in Fig. 4 we have assumed that there is no atomic nitrogen. The sources of NO^+ that are important are $N_2^+ + O$ and $O^+ + N_2$, with $N^+ + O_2$ contributing in the region of more intense precipitation. We have also included

TABLE 1

PRODUCTION	LOSS
[N^+]	
$N_2 + e \rightarrow N^+ + N + 2e$	$N^+ + O_2 \xrightarrow{b_1 k_4} NO^+ + O$
$N + e \rightarrow N^+ + 2e$	$\xrightarrow{b_2 k_4} O_2^+ + N$
$He^+ + N_2 \xrightarrow{k_1} N^+ + N + He$	$N^+ + O \xrightarrow{k_5} N + O^+$
$O^+(^2P) + N_2 \xrightarrow{k_2} N^+ + NO$	
$N(^4S) + O^+(^2P) \xrightarrow{k_3} N^+(^3P) + O(^1S)$ (see text)	
[N_2^+]	
$N_2 + e \rightarrow N_2^+ + 2e$	$N_2^+ + O \xrightarrow{k_8} NO^+ + N$
$N_2 + O^+(^2D) \xrightarrow{k_6} N_2^+ + O$	$N_2^+ + e \xrightarrow{k_9} N + N$
$He^+ + N_2 \xrightarrow{k_1/1.5} N_2^+ + He$	$N_2^+ + O_2 \xrightarrow{k_{10}} O_2^+ + N_2$
$O_2^+(a^4\pi) + N_2 \xrightarrow{k_7} N_2^+ + O_2$	
[$O^+(^2P)$]	
$O + e \rightarrow O^+(^2P) + 2e$	$O^+(^2P) + O \xrightarrow{k_{11}} O^+ + O$
	$O^+(^2P) + N_2 \xrightarrow{k_2} N^+ + NO$
	$O^+(^2P) + e \xrightarrow{k_{12}} O^+(^2D) + e$
	$\xrightarrow{k_{13}} O^+(^4S) + e$
	$O^+(^2P) + N(^4S) \xrightarrow{k_3} O(^1S) + N^+(^3P)$
[$O^+(^2D)$]	
$O + e \rightarrow O^+(^2D) + 2e$	$O^+(^2D) + N_2 \xrightarrow{k_6} N_2^+ + O$
$O^+(^2P) + e \xrightarrow{k_{12}} O^+(^2D) + e$	$O^+(^2D) + e \xrightarrow{k_{14}} O^+(^4S) + e$
$O^+(^2P) \rightarrow O^+(^2D) + h\nu_{7319}$	$O^+(^2D) + N_2 \xrightarrow{k_{21}} NO^+ + N$
[O_2^+]	
$O_2 + e \rightarrow O_2^+ + 2e$	$O_2^+ + e \xrightarrow{k_{16}} O + O$
$N_2^+ + O_2 \xrightarrow{b_1 k_9} O_2^+ + N_2$	$O_2^+ + N \xrightarrow{k_{17}} NO^+ + O$
$N^+ + O_2 \xrightarrow{b_1 k_4} O_2^+ + N$	
$O^+ + O_2 \xrightarrow{k_{15}} O_2^+ + O$	
[$O_2^+(a^4\pi)$]	
$O_2 + e \rightarrow O_2^+(a^4\pi) + 2e$	$O_2^+(a^4\pi) + N_2 \xrightarrow{k_7} N_2^+ + O_2$
	$O_2^+(a^4\pi) + O_2 \xrightarrow{k_{18}} O_2^+(x^2\Pi_g) + O_2$
	$O_2^+(a^4\pi) + e \xrightarrow{k_{19}} O_2^+ + e$
[NO^+]	
$N_2^+ + O \xrightarrow{k_8} NO^+ + N$	$NO^+ + e \xrightarrow{k_{22}} N + O$
$O^+ + N_2 \xrightarrow{k_{20}} NO^+ + N$	
$N^+ + O_2 \xrightarrow{b_1 k_4} NO^+ + O$	
$O_2^+ + N \xrightarrow{k_{17}} NO^+ + O$	
$O^+(^2D) + N_2 \xrightarrow{k_{21}} NO^+ + N$	
[N]	
$N_2 + e \rightarrow N^+ + N + 2e$	$N + O_2 \xrightarrow{k_{23}} NO + O$
$\rightarrow N + N$	$N + NO \xrightarrow{k_{24}} O + N_2$
$He^+ + N_2 \xrightarrow{k_1} N^+ + N + He$	
$N_2^+ + O \xrightarrow{k_8} NO^+ + N$	
$N_2^+ + e \xrightarrow{k_9} N + N$	
$NO^+ + e \xrightarrow{k_{22}} N + O$	
$O^+ + N_2 \xrightarrow{k_{20}} NO^+ + N$	
$N^+ + O_2 \xrightarrow{b_1 k_4} O_2^+ + N$	
$N^+ + O \xrightarrow{k_5} O^+ + N$	

the source of NO^+ from the reaction $O^+(^2D) + N_2 \rightarrow NO^+ + N$ discussed by Torr *et al.*, (1975c). This contributes approximately 20 % in the region of maximum particle energy influx. The only loss of NO^+ is by dissociative recombination. We have used a recombination rate for NO^+ of $4{\cdot}3 \times 10^{-7}$ $(Te/300)^{-0.37}$ (Huang *et al.*, 1975) as this value was found to explain the observed $[NO^+]$ on three night-time orbits under quiet conditions (Torr *et al.*, 1975b). Significant sources of O_2^+ are the charge exchange reactions with O^+ and N^+. Electron impact ionization of O_2 contributes 10 % in the region of maximum electron precipitation (between 26,383 and 26,413 sec UT). An additional loss of O_2^+ is needed in this region. It was also found, in preliminary calculations of the N^+, that we were unable to account for the observed N^+ densities in the absence of atomic nitrogen after 26,363 sec UT. Indications are that the presence of N would provide the required loss process for O_2^+ and the required source for N^+.

Since the chemical lifetime of $N(^4S)$ at 280 km is approx. 4×10^4 sec and the time constant associated with diffusion is ~500 sec, the N densities at these altitudes are diffusively controlled. Thus, we have not calculated the atomic nitrogen densities directly from the N photochemistry, but from the measured ratio of $[NO^+]/[O_2^+]$, where we solve for the [N] required to bring the $[NO^+]$ and $[O_2^+]$ photochemistry into balance, i.e.

$$\frac{[NO^+]}{[O_2^+]} = \frac{(k_{17}[O_2^+][N] + q_2)(k_{16}[e] + (k_{17}[N])}{k_{22}[e]q_1}, \quad (1)$$

where q_1 is the total production of O_2^+ and q_2 is the production of NO^+ due to all sources other than $O_2^+ + N \rightarrow NO^+ + O$.

The resulting N densities are shown in Fig. 5, along with the observed ion densities and those calculated including these N densities in the photochemistry. Using $k_{17} = 1{\cdot}8 \times 10^{-10}$ cm^3 sec^{-1} the maximum [N] obtained in the region of most intense particle precipitation is 7×10^7 cm^{-3}. However, it is likely that a significant fraction of the N will be formed in the ^2D state in which case k_{17} may be 4×10^{-10} cm^3 sec^{-1} (Dalgarno, 1970). These values for [N] are therefore the upper limit. We can calculate the lower limit by assuming that all the N is $N(^2D)$ and find that the maximum density is 2×10^7 cm^{-3}. An estimate of the [NO] from the reactions $N + O_2 \xrightarrow{k_{23}} NO + O$ and $NO + N \xrightarrow{k_{24}} O + N_2$ indicates that [NO] in the region of most intense precipitation would not compete with N in charge exchanging with O_2^+ even if we assume that all the N is $N(^2D)$ and use $k_{23} = 4{\cdot}4 \times 10^{-13}$ $(Tn)^{1/2}$ (Slanger *et al.*, 1971) and $k_{24} = 7{\cdot}0 \times 10^{-11}$ cm^3 sec^{-1} (Black *et al.*, 1969; Lin and Kaufman, 1971).

TABLE 2. RATE COEFFICIENTS, $k(\text{cm}^3\ \text{sec}^{-1})$ AND BRANCHING RATIOS, b

Rate Coefficient	Reference
$k_1 = 1.2\ (-9)$	Lindinger et al. (1974)
$k_2 = 2.5\ (-10)$	Torr et al. (1975a)
$k_3 = 1.7\ (-9)$	Torr et al. (1975a)
$k_4 = 5.0\ (-10)$	Lindinger et al. (1974)
$k_5 = 1.0\ (-12)$	Torr et al. (1975a)
$k_6 = 7.0\ (-10)$	Rutherford and Vroom (1971)
$k_7 = 4.0\ (-10)$	Lindinger et al. (1975)
$k_8 = \begin{cases} 1.4\ (-10)(T_i/300)^{-0.44} \times (1-0.07 \times (T_i/300)^{2.1}) & \text{for } T_i < 1500°K. \\ 5.2\ (-11)(T_i/300)^{0.2} \times (1-0.07 \times (T_i/300)^{2.1}) & \text{for } T_i > 1500°K. \end{cases}$	McFarland et al. (1974)
$k_9 = 1.8\ (-7)(T_i/300)^{0.5}(T_e/300)^{-0.5}$	Mehr and Biondi (1969) Oppenheimer (private communication, 1975)
$k_{10} = 5.0\ (-11)(T_i/300)^{-0.8}$	Lindinger et al. (1974)
$k_{11} = 2.0\ (-10)$	Hays et al. (1975)
$k_{12} = 1.8\ (-7)(300/T_e)^{0.5}$	Henry et al.(1969)
$k_{13} = 2.0\ (-8)$	Henry et al. (1969)
$k_{14} = 3.0\ (-8)$	Henry et al. (1969)
$k_{15} = 1.3\ (-11)(T_i/300)^{-0.4}$	Lindinger et al. (1974)
$k_{16} = \begin{cases} 1.1\ (-5)\ T_e^{-0.7} & \text{for } T_e < 1200°K \\ 3.9\ (-6)\ T_e^{-0.56} & \text{for } T_e > 1200°K \end{cases}$	Biondi (1969)
$k_{17} = 1.8\ (-10)$	Ferguson (1974)
$k_{18} = 3.0\ (-10$	Lindinger et al. (1975)
$k_{19} = 1.0\ (-7)$	Assumed cf. Walker and Rees (1967)
$k_{20} = 6.0\ (-13)$	Lindinger et al. (1974)
$k_{21} = 2.0\ (-10)$	Torr et al. (1975c)
$k_{22} = 4.3\ (-7)(T_e/300)^{-0.37}$	Huang et al.(1975); Torr et al. (1975b)
$k_{23} = 2.4\ (-11)\ \exp\ (-3975.0/T_n)$	Wilson (1967)
$k_{24} = 1.5(-12)\ T_n^{\frac{1}{2}}$.	Phillips and Schiff (1962)
$b_1 = .5$	
$b_2 = .5$	

(b) N_2^+

From Figs. 1 and 5, it can be seen that $[N_2^+]$ increases almost linearly with the increase in electron energy flux. This is because there are only two important sources, both of which increase linearly with the energy flux. These are electron impact on N_2 and the reaction of N_2 with metastable $O^+(^2D)$, where $O^+(^2D)$ is produced by electron impact on O. The $O^+(^2D)$ photochemistry is given in Table 1 and the densities calculated from this are given in Table 3. Between 200 to 260 km, N_2^+ is lost predominantly by $N_2^+ + O \rightarrow NO^+ + N$. Above 260 km (26,364 sec UT) the major loss process is by recombination with electrons.

(c) N^+

Below 260 km (26,360 sec UT) the $[N^+]$ increases in a way very similar to the $[N_2^+]$, but increases more steeply above this point. Over the lower altitude range the sources of N^+ resemble those for N_2^+; they are electron impact on N_2 and $O^+(^2P) + N_2 \rightarrow N^+ + NO$ (Torr *et al.*, 1975a). The $O^+(^2P)$ photochemistry is given in Table 1 and the densities calculated from this are given in Table 3. Above this altitude, as mentioned earlier, we were unable to theoretically reproduce the observed N^+ densities without including atomic nitrogen, the calculated N^+ being too low by a factor of ~3·5. The inclusion of electron impact on N made

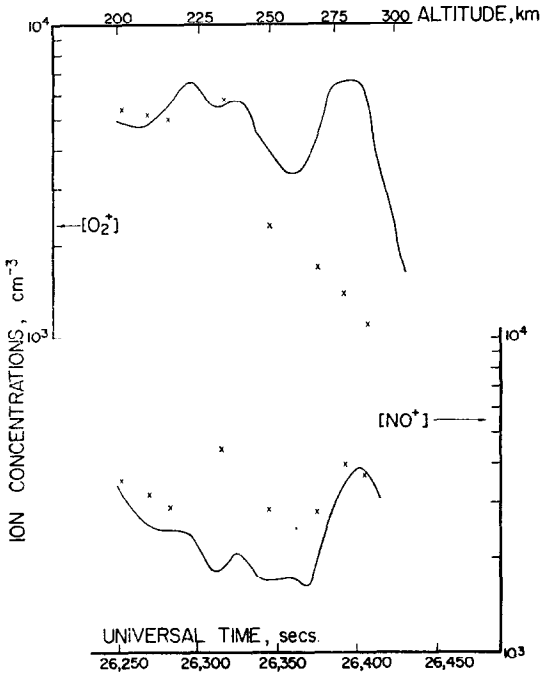

FIG. 4. MEASURED AND CALCULATED DENSITIES OF NO^+ AND O_2^+ AS A FUNCTION OF UT AND ALTITUDE WHEN NO ATOMIC NITROGEN IS INCLUDED IN THE PHOTOCHEMISTRY.

up most of the deficit together with the fast reaction $O^+(^2P) + N(^4S) \rightarrow N^+(^3P) + O(^1S)$ either directly or via $O^+(^2P) + N(^4S) \rightarrow N^+(^1S) + O(^3P)$ followed by the nearly resonant quenching of $N^+(^1S)$ by $O(^3P)$ yielding $N^+(^3P)$ and $O(^1S)$. The rate k_3 given in Table 1 is the total of these two channels (Torr *et al.*, 1975a). These reactions also provided a significant contribution to $O(^1S)$ excitation, as observed by the 5577 Å emission; this will be discussed in Section 6. Figure 6 is a plot of the important N^+ production rates.

TABLE 3

UT sec	Altitude	$[NO^+]/[O_2^+]$	$O^+(^2D)$	$O^+(^2P)$
26250	200	.62	1.2 (0)	9.2 (-1)
26265	206	.64	1.9 (0)	1.4 (0)
26280	214	.60	2.1 (0)	1.4 (0)
26295	221	.58	4.1 (0)	2.4 (0)
26310	229	.61	2.6 (1)	1.4 (1)
26325	237	.91	5.6 (1)	2.6 (1)
26340	246	1.11	6.0 (1)	2.0 (1)
26355	255	0.90	4.7 (1)	1.4 (1)
26370	264	0.90	1.0 (2)	1.7 (1)
26385	274	1.81	2.2 (2)	3.1 (1)
26400	283	3.44	4.3 (2)	5.8 (1)
26415	294	2.00	3.5 (2)	3.9 (1)
26430	304	0.50	2.4 (1)	2.1 (0)

It would appear that the reason for the more dramatic change in N^+ in the region of the most intense particle precipitation is its dependence on N which in turn appears to be enhanced in regions of large energy influx. Since the diffusion time constant for N is much shorter than the photochemical lifetime at ~280 km (the altitude at which the particle detectors saw the largest energy flux), the N density at this altitude must be controlled by processes which occur at altitudes where N is photochemically controlled, followed by upward diffusion. The N density is photochemically

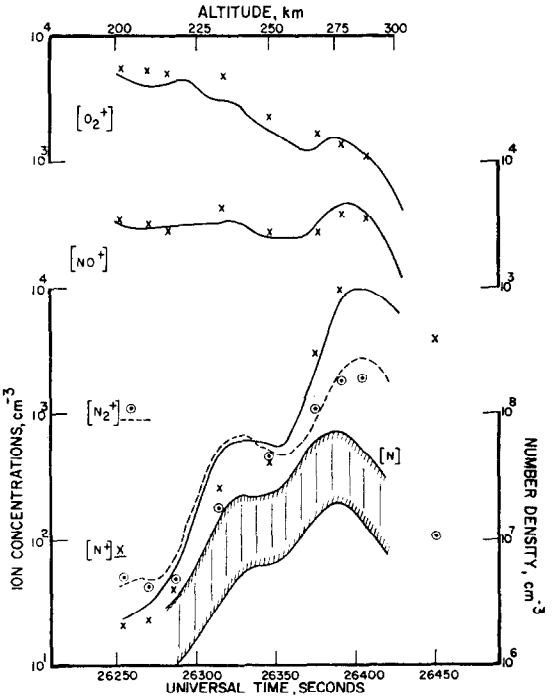

FIG. 5. MEASURED AND THEORETICAL DENSITIES OF O_2^+, NO^+, N^+ AND N_2^+. ATOMIC NITROGEN DENSITIES CALCULATED FROM THE OBSERVED $[NO^+]/[O_2^+]$ RATIO WERE USED IN THE CALCULATION. THE N DENSITIES ARE ALSO SHOWN.

controlled below 200 km and the maximum loss of energy from the fast electrons to the atmosphere takes place below 200 km. Reactions which produce atomic nitrogen are given in Table 1. Below 200 km the main sources of N (electron impact on N_2, dissociative recombination of N_2^+ and NO^+ and the reactions $N_2^+ + O$, $O^+ + N_2$ and $N^+ + O_2$) all depend directly on the energy input. It is unlikely that a single auroral event would persist for long enough to enhance the atomic nitrogen to the levels deduced above. However, since N has a lifetime at *F*-region altitudes of longer than 10^4 sec, it is

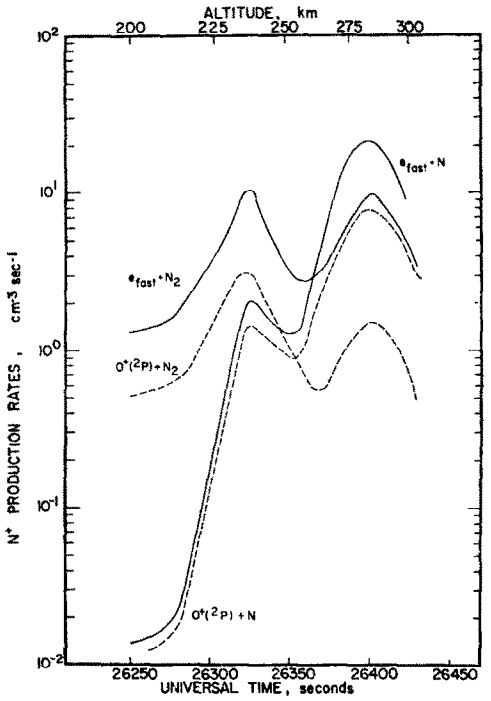

FIG. 6. PRODUCTION RATES OF N^+ DUE TO ELECTRON IMPACT ON N_2 AND ON N, AND DUE TO THE REACTION $O^+(^2P) + N(^4S) \rightarrow O(^1S) + N^+(^3P)$.

possible that atomic nitrogen might be generally enhanced in the auroral oval where there is continual particle energy influx.

An important aspect of the atomic nitrogen enhancements associated with the precipitated electron energy flux is that they cause N to be the dominant constituent responsible for the loss of $O^+(^2P)$.

It is likely that the atomic nitrogen would appear as NO in a neutral mass spectrometer and this may explain the measurements of large NO densities that have been reported in auroras.

As mentioned earlier, the satellite is only able to monitor the precipitated flux at one instant in time at each point along the track and it is possible that large temporal fluctuations may have occurred in the region of more intense precipitation. However, from the good agreement obtained between experiment and theory in this analysis, it appears that this aurora was stable for long enough for the ionosphere to attain a state of chemical equilibrium. This is not surprising since the lifetimes of the molecular ions at 280 km are less than 100 sec and that of N^+ is approx. 200 sec.

We have not attempted a photochemical comparison with O^+ as it is significantly affected by transport over the altitude region we are studying.

The four ions NO^+, O_2^+, N_2^+ and N^+ form a rather tightly knit system so that a significantly wrong reaction rate or density used in determining one, will tend to show up in one or more of the others. This requirement for internal consistency, provides a useful constraint which gives added reliability to the conclusions drawn.

5. ELECTRON AND ION COOLING RATES AND ELECTRIC FIELDS

The processes effective in cooling the electron gas have been discussed in a review paper by Schunk and Walker (1973). The cooling rates due to these processes have been calculated from the measured temperatures and are shown in Fig. 7. As would be expected, the dominant loss process above 300 km is elastic collisions with positive ions; below 300 km cooling occurs mainly by the excitation of the fine structure levels of atomic oxygen. However, the contribution by elastic collisions with ions below 300 km is much larger than in non-auroral conditions where the ion densities are not

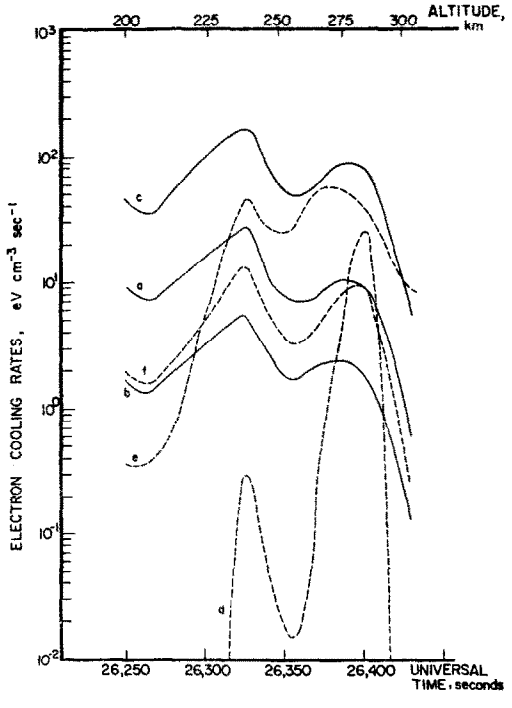

FIG. 7. ELECTRON COOLING RATES AS A FUNCTION OF ALTITUDE AND UT DUE TO (a) ROTATIONAL EXCITATION OF N_2, (b) ROTATIONAL EXCITATION OF O_2, (c) FINE STRUCTURE LEVELS OF ATOMIC OXYGEN (d) EXCITATION OF $O(^1D)$, (e) COULOMB COLLISIONS WITH POSITIVE IONS (f) ELASTIC COLLISIONS WITH NEUTRALS.

enhanced (see, e.g. Dalgarno, 1969). Cooling by excitation of the ^1D metastable state of atomic oxygen is important during the precipitation event in the vicinity of 283 km (26,415 sec UT). Cooling due to elastic collisions with neutrals and due to rotational excitation of O_2 are not entirely negligible and contribute up to 5% of the total cooling.

The ion gas is cooled by elastic ion-neutral interactions and resonant charge exchange between ions and their parent neutrals. The cooling rates due to these two processes are shown in Fig. 8. The rates are reasonable but they are sensitive to the values we have assumed for T_n.

If we neglect thermal conduction (which is probably not significant at these altitudes) we can solve for the perpendicular electric field, $E_\perp$, in the aurora by equating the Joule heating rate to the ion-neutral cooling rate. The relevant expressions are given in Schunk and Walker (1973). The values thus obtained for $E_\perp$ along the satellite track are shown in Fig. 8. The maximum perpendicular electric field obtained is 27 mV/m. This would correspond to a horizontal ion drift of 540 m/sec. It would therefore appear that in this aurora, electrodynamic transport of the ions is not significant.

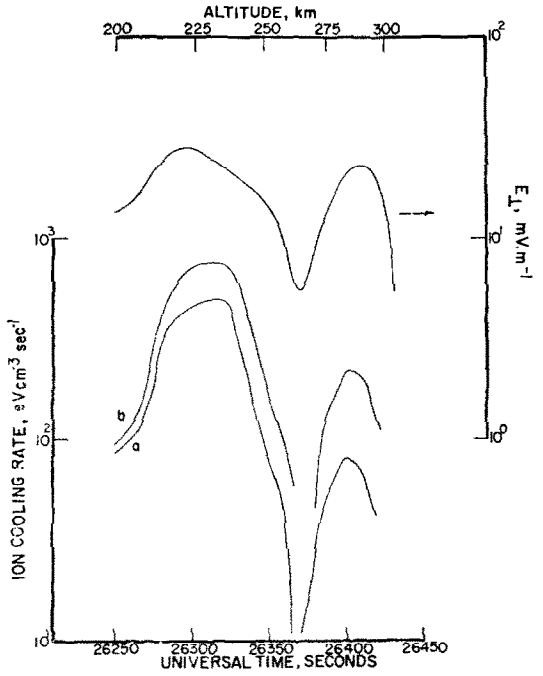

FIG. 8. ION COOLING RATES AS A FUNCTION OF ALTITUDE AND UT DUE TO (a) ELASTIC COLLISIONS WITH NEUTRALS (b) RESONANT CHARGE TRANSFER. ALSO SHOWN IS THE PERPENDICULAR ELECTRIC FIELD CALCULATED BY EQUATING THE TOTAL ION COOLING RATE TO THE JOULE HEATING RATE.

Also because the ion drifts in this case are relatively small the NO^+ density would not be enhanced due to the increase in the rate coefficient of the reaction $O^+ + N_2 \rightarrow NO^+ + N$ with ion velocity (Banks *et al.*, 1974).

6. COMPARISON WITH OPTICAL EMISSIONS

The visible airglow emissions on the AE-C satellite are measured by the photometer described by Hays *et al.* (1973). On this orbit the photometer was observing 6300 Å on the wide channel (3° half-angle) and 5577 Å on the narrow channel (0·75° half-angle). The upward looking surface brightness at 6300 Å is shown in Fig. 1.

In the case of high spatial structure in the emissions, such as occurs through this aurora, it is very difficult to obtain volume emission rates along the path of the satellite. We have attempted in this case to obtain volume emission rates for comparison with those calculated in the following way.

Because the satellite is spinning, we have surface brightnesses looking both horizontally and vertically. If we assume that the temporal variations are not severe in a quarter revolution (4 sec) and that the vertical volume emission rates are exponential with altitude we can write

$$I_H/I_U = \mathrm{Ch}(90°), \tag{2}$$

where I_H = horizontal surface brightness; I_U = upward surface brightness and Ch (90°) is the Chapman function looking at 90° through the atmosphere. Having the Chapman function, we can solve for the scale height, H, of the 6300 Å emission from

$$\mathrm{Ch}(90°) = \left[\frac{\pi R}{2H}\right]^{1/2}, \tag{3}$$

where R is the altitude of the satellite above the center of the Earth.

In Fig. 9 we have shown the horizontal surface brightness at 6300 Å looking both backward and forward along the satellite track. The upward surface brightness is shown in Fig 1.

As this approximation to the Chapman function assumes spherical symmetry, it would appear from these data that there are only two points at which the above technique will provide volume emission rates that can reasonably be compared with those calculated. These are at the maxima in the upward looking surface brightness at 26,324 and 26,415 sec UT, since at these maxima the horizontal channels will be seeing mainly the local bright emission and

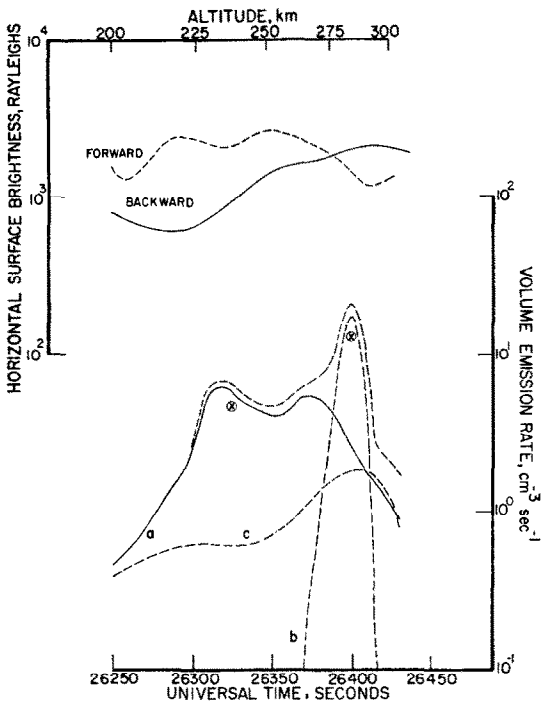

FIG. 9. HORIZONTAL 6300 Å SURFACE BRIGHTNESS LOOKING FORWARD AND BACKWARD ALONG THE TRACK. ALSO SHOWN ARE THE CALCULATED 6300 Å VOLUME EMISSION RATES DUE TO (a) DISSOCIATIVE RECOMBINATION OF O_2^+, (b) THERMAL ELECTRON EXCITATION AND (c) FAST ELECTRONS. THE TWO VOLUME EMISSION RATES DEDUCED FROM THE PHOTOMETER OBSERVATIONS ARE SHOWN FOR COMPARISON.

not distant emissions. Before 26,309 sec UT the horizontal channels are either looking back into dimmer regions or forward into brighter regions than would correspond to the locally overhead situation. Between these two altitudes the satellite is passing through a dim region between two bright regions and after 26,415 sec UT the forward channel looks into dawn while the backward channel still sees the bright aurora behind.

We have therefore taken the average of the backward and forward horizontal counts at 26,324 and 26,415 sec UT and have derived volume emission rates at these two points. We have calculated the $O(^1D)$ volume emission rates due to (1) disociative recombination, (2) thermal electron excitation and (3) secondary electron impact excitation where

$$\eta_1 = [O_2^+][e]k_{17}/q, \tag{4}$$

$$q = \frac{A_{6300}}{A(^1D)}\Big/(1 + \beta[N_2]/A(^1D)), \tag{5}$$

$$\beta = 5 \times 10^{-11}\ \text{cm}^3\ \text{sec}^{-1}, \tag{6}$$

$$\eta_2 = 1{\cdot}1 \times 10^{-10} \times [e] \times [O] \times T_e^{1/2} \times \exp(-2{\cdot}27 \times 10^4/T_e) \times [0{\cdot}406 + 0{\cdot}357 \times 10^{-4}T_e - (0{\cdot}333 + 0{\cdot}183 \times 10^{-4}T_e) \times \exp(-1{\cdot}37 \times 10^4/T_e) - (0{\cdot}456 + 0{\cdot}174 \times 10^{-4}T_e) \times \exp(-2{\cdot}97 \times 10^4/T_e)]/q$$

(Rees *et al.*, 1967), (7)

and

$$\eta_3 = [O]\int_{E_{th}}^{\infty} \sigma_{O(^1D)}(E)\,\phi(E)\,dE/q. \tag{8}$$

These are shown in Fig. 9 with the two volume emission rates deduced from the observations shown for comparison. Below 10 eV where the shielding effects of the local plasma generated by the spacecraft affected data from half the spin cycle (Doering *et al.*, 1975), it is possible that the electron fluxes used here are too low. However, it would appear that the 6300 Å emission can be almost entirely accounted for by dissociative recombination in the diffuse auroral region and by thermal excitation in the region of field aligned precipitation, i.e. 26,309–26,380 sec UT and 26,385–26,420 sec UT respectively.

On this orbit the F-region 5577 Å emission is just detectable above the galactic background in the regions of electron precipitation and some 20–40 R of this emission was seen in the upward direction (corresponding to 2 or 3 counts per integration period above the dark count and galaxy). In the region of diffuse precipitation this results from the dissociative recombination of O_2^+, which also produces the 6300 Å emission. However, in the region of intense precipitation centered on ~283 km (26,415 sec UT) the $O(^1D)$ is accounted for by thermal excitation and this could not produce $O(^1S)$. Charge exchange of $O^+(^2P)$ with $N(^4S)$ as discussed earlier, contributes significantly to the production of N^+ in this region, and this process would also produce $O(^1S)$ at a rate of 5·0 $cm^{-3}\ sec^{-1}$. If we attempt to estimate the volume emission rate of 5577 Å emission from the photometer observations in the same way as we have done for the red line, we obtain a value of 3·5 $cm^{-3}\ sec^{-1}$ at 26,415 UT. This could vary by a factor of two due to the uncertainties involved.

These data are clearly not optimum for evaluating the $O(^1S)$ production arising from this reaction and we shall do this more accurately elsewhere. However, the indications are that the process could be a significant source of $O(^1S)$ at high altitudes.

CONCLUSIONS

From the agreement obtained between the observed NO^+, O_2^+ N_2^+ and N^+ densities and those calculated from photochemical theory, it would appear that transport effects and time variations are not the dominant factors controlling these ions in this aurora in the altitude range 200–300 km. Quantitative photochemical studies of ions in auroras measured by a satellite may therefore be easier than was anticipated. The internal consistency demanded by the system of simultaneously measured ions provides a useful constraint on the photochemistry.

Although the uncertainties introduced by the low resolution of the ion data do not allow us to establish the density with certainty, it emerges from the study that atomic nitrogen is enhanced in regions of intense particle precipitation, and that atomic nitrogen plays an important role in the photochemistry. The major source of N^+ is electron impact on N, the balance being provided by electron impact on N_2 and the fast reactions

$$O^+(^2P) + N(^4S) \rightarrow O(^1S) + N^+(^3P)$$
$$\rightarrow O(^3P) + N^+(^1S).$$

These reactions could provide a significant source of $O(^1S)$ in precipitation events at these altitudes. The atomic nitrogen also becomes the dominant constituent responsible for the removal of $O^+(^2P)$ in the region of most intense energy influx.

Acknowledgements—We wish to thank all members of the Atmosphere Explorer team, whose co-operation and support provided the data for this study. This work was supported in part by NASA Contract NAS 5-20705 to Cornell University. We are grateful to P. B. Hays for the airglow measurements, to L. R. Brace for the electron temperatures, to A. O. Nier for neutral density measurements, and to D. W. Rusch for reading the manuscript.

REFERENCES

Banks, P. M. and Kockarts, G. (1973). *Aeronomy*. Academic Press, New York.

Banks, P. M., Schunk, R. W. and Raitt, W. J. (1974). NO^+ and O^+ in the high latitude *F*-region. *Geophys. Res. Lett.* **1**, 239–242.

Biondi, M. A. (1969). Atmospheric electron–ion and ion–ion recombination processes. *Can. J. Chem.* **47**, 1711–1719.

Black, G., Slanger, T. C., St. John, G. A. and Young, R. A. (1969). Vacuum-ultraviolet photolysis of N_2O, 4, deactivation of $N(^2D)$ *J. Chem. Phys.* **51**, 116–121.

Brace, L. H., Thesis, R. G. and Dalgarno A. (1973). The cylindrical electrostatic probes for Atmosphere Explorer -C, -D and -E. *Radio. Sci.* **8**, 341–348.

Dalgarno. A. (1969). Inealstic collisions at low energies. *Can. J. Chem.* **47**, 1723–1729.

Dalgarno, A. (1970). Metastable species in the ionosphere. *Ann. Geophys.* **26**, 601–607.

Dalgarno, A. and Lejeune, G. (1971). The absorption of electrons in atomic oxygen. *Planet. Space Sci.* **19**, 1653–1667.

Dalgarno, A., Hanson, W. B., Spencer, N. W. and Schmerling, E. R. (1973). The Atmosphere Explorer mission. *Radio Sci.* **8**, 263–267.

Doering, J. P., Bostrom, C. O. and Armstrong, J. C. (1973). The photoelectron-spectrometer experiment on Atmosphere Explorer. *Radio Sci.* **8**, 387–392.

Doering, J. P., Peterson, W. K., Bostrom, C. O. and Armstrong, J. C. (1975). Measurement of low energy electrons in the day airglow and dayside auroral zone from Atmosphere Explorer-C. *J. geophys. Res.* In press.

Donahue, T. M., Zipf, E. C. and Parkinson. T. D. (1970). Ion composition and ion chemistry in an aurora. *Planet. Space Sci.* **18**, 171–186.

Fehsenfeld, F. C., Dunkin, D. B. and Ferguson, E. E. (1970). Rate constants for the reaction of CO_2^+ with O, O_2 and NO; N_2^+ with O and NO; and O_2^+ with NO. *Planet. Space Sci.* **18**, 1267–1269.

Ferguson, E. E. (1974). Laboratory measurements of ionospheric ion-molecule reaction rates. *Rev. Geophys. Space Phys.* **12**, 703–714.

Hanson, W. B., Zuccaro, D. R., Lippincott, C. R. and Sanatani, S. (1973). The retarding potential analyser on Atmosphere Explorer. *Radio Sci.* **8**, 333–340.

Hays, P. B., Carignan, G. R., Kennedy, B. C., Shepherd, G. G. and Walker, J. C. G. (1973). The visible-airglow experiment on Atmosphere Explorer. (1973). *Radio Sci.* **8**, 369–378.

Hays, P. B., Jones, R. A. and Rees, M. H. (1974). Auroral heating and the composition of the neutral atmosphere. *Planet. Space Sci.* **21**, 559–574.

Hays, P. B., Rusch, D. W., Torr, D. G., Sharp, W. E. and Swenson, G. R. (1975). Production and loss of $O^+(^2P)$ ions in the dayglow and the aurora, *EOS*. In press.

Henry, R. J. W., Burke, P. G. and Sinfailam, A. L. (1969). Scattering of electrons by C, N, O, N^+, O^+ and O^{++}. *Phys. Rev.* **178**, 218–225.

Hoffman, J. H., Hanson, W. B., Lippincott, C. R. and Ferguson, E. E. (1973). The magnetic ion–mass spectrometer on Atmosphere Explorer. *Radio Sci.* **8**, 315–322.

Hoffman, R. A., Burch, J. L., Janetzke, R. W., McChesney, J. F., Way, S. H. and Evans, D. S. (1973). Low-energy electron experiment for Atmosphere Explorer-C and -D. *Radio Sci.* **8**, 393–400.

Huang, C. M., Biondi, M. A. and Johnsen, R. (1975). Variation of electron–NO^+–ion recombination coefficient with electron temperature. *Phys. Rev.* **11A**, 901–905.

Jones, R. A. and Rees, M. H. (1973). Time dependent studies of the aurora—I. Ion density and composition. *Planet. Space Sci.* **21**, 537–557.

Kieffer, L. J. and Dunn, G. H. (1966). Electron impact ionization cross section data for atoms, atomic ions and diatomic molecules: I. Experimental data. *Rev. Mod. Phys.* **38**, 1.

Lin, C. L. and Kaufman, F. (1971). Reactions of metastable nitrogen atoms. *J. Chem. Phys.* **55**, 3760–3770.

Lindinger, W., Fehsenfeld, F. C. Schmeltekopf, A. L.

and Ferguson, E. E. (1974). Temperature dependence of some ionospheric ion-neutral reactions from 300° to 900°K. *J. geophys. Res.* **79**, 4753–4756.

Lindinger, W., Albritton, D. L., McFarland, M., Fehsenfeld, F. C. Schmeltekopf, A. L. and Ferguson, E. E. (1975). Rate constants for the reactions of $O_2^+(a^4\pi_u)$ ions with N_2, Ar, CO, CO_2, H_2 and O_2 at relative kinetic energies 0·04 to 2eV. *J. Chem. Phys.* In press.

McFarland, M., Albritton, D. L., Fehsenfeld, F. C., Ferguson, E. E. and Schmeltekopf, A. L. (1974). Energy dependence and branching ratio of the $N_2^+ + O$ reaction, *J. geophys. Res.* **79**, 2925–2926.

Mehr, F. J. and Biondi, M. A.(1969). Electron temperature dependence of recombination of O_2^+ and N_2^+ ions with electrons. *Phys. Rev.* **181**, 264–271.

Narcisi, R. S., Sherman, C., Wlodyka, L. E. and Ulwick, J. C. (1974). Ion composition in an IBC class II aurora 1. Measurements. *J. geophys. Res.* **79**, 2843–2848.

Nier, A. O., Potter, W. E., Hickman, D. R. and Mauersberger, K. (1973). The open-source neutral-mass spectrometer on Atmosphere Explorer-C, -D and -E. *Radio Sci.* **8**, 271–276.

Nier, A. O., Potter, W. E., Kayser, D. C. and Finstad, R. G. (1974). The measurements of chemically reactive atmospheric constituents by mass spectrometers carried on high-speed spacecraft. *Geophys. Res. Lett.* **1**, 197–199.

Nier, A. O., Potter, W. E., Kayser, D. C. and Finstad, R. G. (1974). Neutral atmospheric composition at 200 km near 65°N in Spring, 1974, *EOS* **56**, 1162.

Phillips, L. F. and Schiff, H. I. (1962). Mass spectrometric studies of atom reactions I. Reactions in the atomic nitrogen–ozone system. *J. Chem. Phys.* **36**, 1509–1517.

Rapp, D. and Englander-Golden, P. (1965). Total cross-sections for ionization and attachment in gases by electron impact. I. Positive ionization. *J. Chem. Phys.* **43**, 1464–1479.

Rees, M. H., Walker, J. C. G. and Dalgarno, A. (1967). Auroral excitation of the forbidden lines of atomic oxygen. *Planet. Space Sci.* **15**, 1097–1110.

Rutherford, J. A. and Vroom, D. A. (1971). Effect of the metastable $O^+(^2D)$ on reactions of O^+ with nitrogen molecules. *J. Chem. Phys.* **55**, 5622–5624.

Schram, B. L., DeHeer, F. J., Van der Wiel, M. J. and Kistemaker, J. (1965). Ionization cross sections for electrons (0·6–20 KeV) in noble and diatomic gases. *Physica* **31**, 94–112.

Schram, B. L., Moustafa, H. R., Schutten, J. and DeHeer F. J. (1966). Ionization cross sections for electrons (100–600 KeV) in noble and diatomic gases. *Physica.* **32**, 734–740.

Schunk, R. W. and Walker, J. C. G. (1973). The theory of charged particle temperatures in the upper atmosphere, *Progress in High Temperature Physics and Chemistry* (Ed. C. A. Rouse), Vol. 5, pp. 1–62. Pergamon Press, Oxford.

Slanger, T. G., Wood, B. J. and Black, G. (1971). Temperature coefficient for $N(^2D)$ quenching by O_2 and N_2O. *J. geophys. Res.* **76**, 8430.

Spencer, N. W., Niemann, H. B. and Carignan, G. R. (1973). The neutral atmosphere temperature instrument. *Radio. Sci.* **8**, 284–296.

Swider, W., Jr. and Narcisi, R. S. (1970). On the ionic constitution of class I auroras. *Planet. Space Sci.* **18**, 378–385.

Swider, W., Jr. and Narcisi, R. S. (1974). Ion composition in an IBC class II aurora, 2, model. *J. geophys. Res.* **79**, 2849–2852.

Tate, S. H. and Smith, P. T. (1932). The efficiencies of ionization and ionization potentials of various gases under electron impact. *Phys. Rev.* **39**, 270–277.

Torr, D. G., Rusch, D. W., Hanson, W. B., Hays, P. B., Hoffman, J. H., Torr, M. R. and Walker, J. C. G. (1975a). Reactions of metastable species as sources of atomic nitrogen ions in the thermosphere. Submitted to *J. geophys. Res.*

Torr, M. R., Burnside, R. G., Hays, P. B., Stewart, A. I., Torr, D. G. and Walker, J. C. G. (1975b) Metastable ^2D atomic nitrogen in the nocturnal ionosphere. Submitted to *J. geophys. Res.*

Torr, D. G., Hays, P. B., Rusch, D. W., Torr, M. R. and Walker, J. C. G. (1975c) Atomic nitrogen densities in the thermosphere. Submitted to *Geophys. Res. Lett.*

Walker, J. C. G. and Rees, M. H.(1968) Ionospheric electron densities and temperatures in aurora. *Planet. Space Sci.* **16**, 459–475.

Wilson, W. E. (1967) Rate constant for the reaction $N + O_2 \rightarrow NO + O$. *J. Chem. Phys.* **46**, 2017–2018.